

9<sup>th</sup> International Conference on Photonic Technologies - LANE 2016

## Investigations on laser beam welding of different dissimilar joints of steel and aluminum alloys for automotive lightweight construction

Oliver Seffer<sup>a,\*</sup>, Ronny Pfeifer<sup>a</sup>, André Springer<sup>a</sup>, Stefan Kaierle<sup>a</sup>

<sup>a</sup>Laser Zentrum Hannover e.V., Hollerithallee 8, 30419 Hannover, Germany

---

### Abstract

Due to the enormous potential of weight saving, and the consequential reduction of pollutant emissions, the use of hybrid components made of steel and aluminum alloys is increasing steadily, especially concerning automotive lightweight construction. However, thermal joining of steel and aluminum is still being researched, due to a limited solubility of the binary system of iron and aluminum causing the formation of hard and brittle intermetallic phases, which decrease the strength and the formability of the dissimilar seam.

The presented results show the investigation of laser beam welding for joining different dissimilar hybrid components of the steel materials HX220LAD+Z100, 22MnB5+AS150 and 1.4301, as well as the aluminum alloy AA6016-T4 as a lap joint. Among other things, the influences of the energy per unit length, the material grade, the sheet thickness  $t$ , the weld type (lap weld, fillet weld) and the arrangement of the base materials in a lap joint (aluminum-sided irradiation, steel-sided irradiation) on the achievable strengths are analyzed. The characterization of the dissimilar joints includes tensile shear tests and metallographic analyses, depending on the energy per unit length.

© 2016 The Authors. Published by Elsevier B.V. This is an open access article under the CC BY-NC-ND license (<http://creativecommons.org/licenses/by-nc-nd/4.0/>).

Peer-review under responsibility of the Bayerisches Laserzentrum GmbH

*Keywords:* dissimilar joints; steel-aluminum; intermetallic phases; laser beam welding; automotive lightweight construction

---

### 1. Introduction and Motivation

In 1993 the Council of the European Union (1993) has adopted a resolution for a decrease of the pollutant emissions of 20 % compared with the emissions of 1990 until the year 2020. Because the traffic causes 26 % of the

---

\* Corresponding author. Tel.: +49-511-2788-483 ; fax: +49-511-2788-100 .  
E-mail address: [o.seffer@lzh.de](mailto:o.seffer@lzh.de)

total emissions of carbon dioxide (CO<sub>2</sub>) in the European Union (EU) and the automobile traffic represents 46 % of them, the average CO<sub>2</sub> emission of new vehicles should be reduced to 95 g/km until the year 2020.

Due to the direct relation between the fuel consumption and the amount of CO<sub>2</sub> emission, the automotive industry has been focused on the development of different approaches for decreasing the fuel consumption. In addition to a decrease of the driving resistance and an increase of the energy efficiency of the engines, the weight reduction of the vehicles and accordingly lightweight construction are of particular importance. As a result of steadily increasing requirements for comfort and driving dynamics, the approaches for lightweight construction are mostly applied in the frame and body construction.

Hybrid constructions of steel and aluminum alloys cause a demand for loadable dissimilar joints and appropriated joining technologies, respectively. Therefore, several joining methods for hybrid components of steel and aluminum alloys are available. Due to an increasing importance of industrial automation and accessibility for frame and body constructions with steadily increasing complexities, the laser beam welding is an appropriate joining technology for these applications. Because the laser beam welding is a thermal joining method, this technology entails metallurgical challenges besides its advantages. Thermal joining methods for dissimilar joints of steel and aluminum alloys cause the formation of hard and brittle intermetallic phases, due to a limited solubility of the binary system of iron and aluminum, which decrease the strength and the formability of the dissimilar seam. Diffusion processes are already affecting the mixing ratios of aluminum to iron of solid-state materials, whereby these effects are much higher for liquid-state materials. As a consequence of the negative influences of the intermetallic phases on the strength and the formability of dissimilar seams, their formation should be prevented as far as possible.

#### Nomenclature

b	weld width
CO <sub>2</sub>	carbon dioxide
EU	European Union
GMAW	gas metal arc welding
λ	wavelength
P <sub>L</sub>	laser beam power
t	sheet thickness
t <sub>E</sub>	penetration depth
t <sub>E, Al</sub>	penetration depth in aluminum alloy
v	welding speed
z	focal position

## 2. State of the Art

Before the development of efficient thermal joining methods, the manufacturing technology in the automotive industry for the joining of dissimilar materials was dominated by mechanical joining methods, e. g. rivetting (blind riveting and punch rivetting), clinching and screwing, as mentioned by Horst (2013) and Büdgam et al. (2004). Some mechanical joining methods as rivetting or screwing require additional components and entail partially a both-sided accessibility to the joining zone.

Furthermore, adhesive bonding methods are favourable joining technologies for dissimilar materials, among other things due to the relatively low process temperatures. The adhesive utilized are based on different polymers in dependence on the application and consists often of epoxy resin or methacrylate, as mentioned by Horst (2013), or of caoutchouc or polyurethanes for the automotive industry, as mentioned by Thomas et al. (2004). An essential disadvantage of adhesive bonding is the requirement for a fixing of the joint partner during the hardening process of the adhesive, as mentioned by Jost et al. (2007). In addition, the adhesive bonding methods are often combined with other joining methods, e. g. resistance spot welding, as mentioned by Arndt et al. (2013), blind riveting, punch riveting or screwing, as mentioned by Thomas et al. (2004), and are termed as hybrid joining.

As a solid-state welding process, the friction stir welding is also a favourable joining technology for dissimilar

materials. However, the tools and clamping devices for friction stir welding are exposed to high wear and tear, due to relatively high process forces, which have to be absorbed by the clamping device with a robust design. Furthermore, typical welding speeds  $v$  required for friction stir welding are relatively low in comparison to other joining technologies with the result of relatively long process times, as shown by Appel and Cramer (2008), Watanabe et al. (2006), Schilling and Strombeck (2005) and Jiang and Kovacevic (2004).

Besides mechanical and solid-state joining technologies, the application of thermal joining methods increases steadily for different joint assignments, especially in the automotive industry. As a result of extensive research activities and fundamental developments, the thermal joining of dissimilar joints of steel and aluminum alloys has been proven for different thermal joining technologies. These thermal joining technologies are the laser beam soldering and brazing, as shown by Nothdurft et al. (2016) and Dorn et al. (2003), the laser beam braze welding, as mentioned by Müller et al. (2005), the laser beam welding, e. g. proven by Kaierle et al. (2014), Kallage (2013), Schilf et al. (2007) and Sierra et al. (2007), the gas metal arc welding (GMAW), as shown by Aichele (2008) and Staubach et al. (2007), the electron beam welding, as mentioned by Lau (2006), and the laser-GMA hybrid welding, as proven by Michailov et al. (2011) and Thomy et al. (2008). Especially, laser-based joining methods are favourable for dissimilar joining of steel and aluminum-alloys, due to their relatively low and controllable heat inputs.

### 3. Experimental Setup and Materials used

Below, the experimental setups used for the laser beam welding of different dissimilar joints of steel and aluminum alloys by steel-sided irradiation and aluminum-sided irradiation, respectively, are presented in Sec. 3.1 and the materials used are mentioned in Sec. 3.2.

#### 3.1. Experimental Setup for the Laser Beam Welding of different dissimilar Joints of Steel and Aluminum Alloys

The laser beam source used for the laser beam welding of different dissimilar joints was a diode-pumped, solid-state disk laser Trumpf TruDisk 16002, with a maximum laser beam power  $P_L$  of 16 kW, a brilliant beam quality of minimum 8 mm·mrad and a wavelength  $\lambda$  of 1,030 nm. The laser beam welding head utilized was a Scansonic BO-SF with a focal length of 250 mm and a collimation length of 120 mm. In addition, the BO-SF welding optic was expanded by a laser beam scanner BO-SF-SCAN-EGY-D-4W-2.1-F250. In combination with an optical fibre with a diameter of 400  $\mu\text{m}$ , a focal spot diameter of about 830  $\mu\text{m}$  results. The laser beam welding head was mounted on a six-axis robot system Kuka KR 60 HA.

The investigations on the laser beam welding of different dissimilar joints of steel and aluminum alloys were operated by using a laser beam power  $P_L$  of 3.75 kW and by setting the focal position  $z$  of the laser beam onto the upperside of the sheet of the aluminum alloy for dissimilar lap welds with steel-sided irradiation as well as aluminum-sided irradiation. The experimental setup used for the steel-sidedly laser beam welding of different dissimilar lap welds of steel and aluminum alloys and a schematic illustration of setting the focal position  $z$  of the laser beam for steel-sided irradiation are shown in Fig. 1.

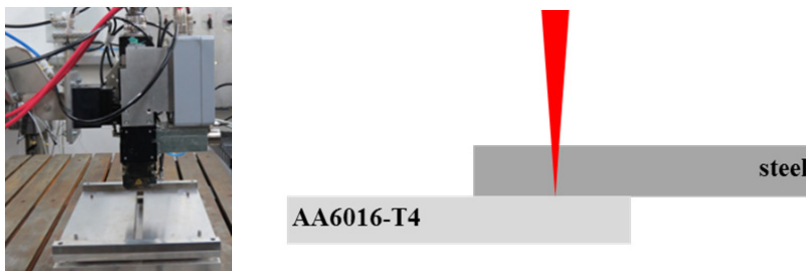


Fig. 1. Experimental setup for the laser beam welding of different dissimilar lap welds of steel and aluminum alloys (steel-sided irradiation).

The clamping device used for the joining of dissimilar lap welds of steel and aluminum alloys by steel-sided irradiation as well as aluminum-sided irradiation is shown in Fig. 2.

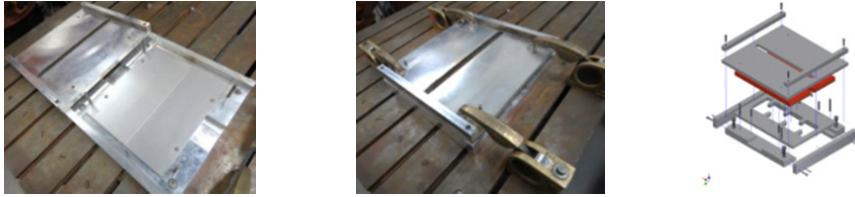


Fig. 2. Clamping device for the laser beam welding of different dissimilar lap welds of steel and aluminum alloys.

During the subsequently presented investigations, the arrangement of the base materials in a lap joint (irradiation direction) as well as the weld type are varied. Thereby, the weld type was modified from lap weld to fillet weld during the investigations on aluminum-sidedly welded dissimilar joints, due to a higher suitability for this joining assignment. The higher suitability of fillet welds is based on the possibilities for a limitation of the amount of melted aluminum alloy and as a consequence for a better control of the mixing ratios of aluminum to iron in the weld metal. Hence, the formation of intermetallic phases and cracks decreases. For the realization of joining dissimilar fillet welds, the axis of laser beam requires an positioning by using relatively high irradiation angles, with the result of a requirement for a modification of the clamping device. These investigations were operated by centrally setting the focal position  $z$  of the laser beam into the fillet between the sheets of the two joint partners. The experimental setup modified for the aluminum-sidedly laser beam welding of different dissimilar fillet welds of aluminum alloys and steel and a schematic illustration of setting the focal position  $z$  of the laser beam for aluminum-sided irradiation are shown in Fig. 3.

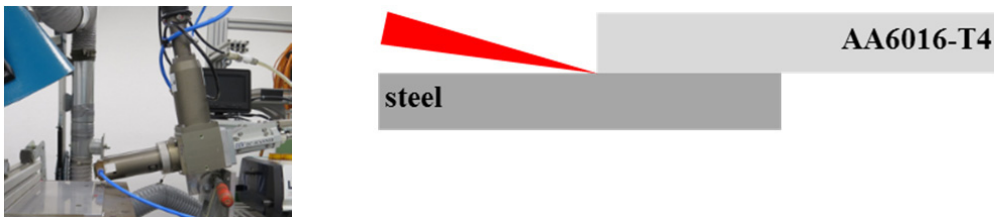


Fig. 3. Experimental setup for the laser beam welding of different dissimilar fillet welds of aluminum alloys and steel (aluminum-sided irradiation).

### 3.2. Materials used

The materials used for the investigations on laser beam welding of different dissimilar joints of steel and aluminum alloys were the steel materials HX220LAD+Z100, 22MnB5+AS150 and 1.4301, as well as the aluminum alloy AA6016-T4. The sheet thickness  $t$  for the samples of the zinc-coated, micro-alloyed, fine-grain structural steel HX220LAD+Z100 was 1.00 mm. In addition, for the laser beam welding of material pairings with the zinc-coated steel, a gap width of 0.10 mm between the joint partners was set to enable the possibility for an outgassing of occurrent zinc vapour. For the ultra high strength steel for hot stamping 22MnB5+AS150, presshardened sheets with a sheet thickness  $t$  of 1.50 mm were used. The sheet thickness  $t$  for the samples of the austenitic chromium-nickel steel 1.4301 was 1.50 mm and 1.15 mm for the samples of the aluminum alloy AA6016-T4, respectively. A sample size for each material of 300.00 mm x 142.50 mm and a lap width of 35.00 mm were used.

#### 4. Evaluation Procedure

Within the scope of the development of the laser beam welding process for different dissimilar joints of steel and aluminum alloys, the influences of the energy per unit length, the material grade, the sheet thickness  $t$ , the weld type (lap weld, fillet weld) and the arrangement of the base materials in a lap joint (aluminum-sided irradiation, steel-sided irradiation) among other things on the achievable strengths are analyzed. The characterization of the dissimilar joints includes metallographic analyses and tensile shear testing, depending on the energy per unit length.

The metallographic analyses of cross-sections contain the evaluation regarding the occurrence of weld imperfections as well as the determination of the weld width  $b$  and the penetration depth in aluminum alloy  $t_{E, Al}$  in dependence on the energy per unit length, the material grade, the sheet thickness  $t$ , the weld type (lap weld, fillet weld) and the arrangement of the base materials in a lap joint (aluminum-sided irradiation, steel-sided irradiation). As a consequence of an etching process within the scope of a metallographic sample preparation, the microstructure of the weld metal, the heat affected zone, the base material and intermetallic phases appear differently in terms of colour.

The tensile shear testing was operated according to EN ISO 14273 with a testing speed of 10 mm/min and by using tensile shear samples with a width of 22.5 mm, a length of 250 mm and an lap width of 35 mm. For each parameter configuration investigated within the tensile shear testing, an amount of five tensile shear samples were tested.

#### 5. Results and Discussion

Below, the results of the metallographic analyses of different laser beam welded dissimilar joints of steel and aluminum alloys are presented in Sec. 5.1 and in Sec. 5.2 the results of the tensile shear testing are mentioned. A typical picture of a process monitoring camera of a laser beam welding process for the joining of different dissimilar joints of steel and aluminum alloys are exemplarily shown in Fig. 4.



Fig. 4. Laser beam welding of different dissimilar joints of steel and aluminum alloys.

In Fig. 5 face of weld of different steel-sidedly laser beam welded dissimilar joints of steel and aluminum alloys, joined by using different steel materials (HX220LAD+Z100, 1.4301 and 22MnB5+AS150) and the process parameters denoted in the previous Sec. 3.1, are exemplarily shown.

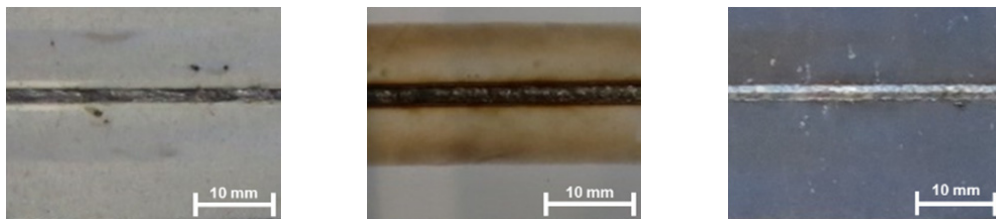


Fig. 5. Face of weld of different steel-sidedly laser beam welded dissimilar joints of steel and aluminum alloys: HX220LAD+Z100 and AA6016-T4 [left], 1.4301 and AA6016-T4 [center] and 22MnB5+AS150 and AA6016-T4 [right].

Face of weld of different aluminum-sidedly laser beam welded dissimilar joints of aluminum alloys and steel, joined by using different weld types (lap weld and fillet weld) and the process parameters denoted in the previous Sec. 3.1, are exemplarily shown in Fig. 6.

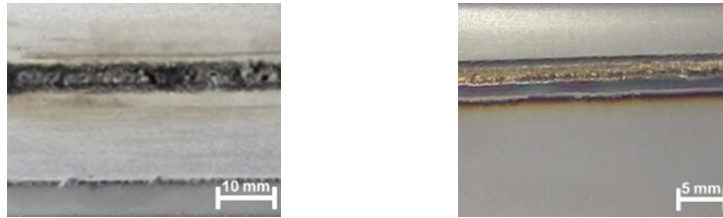


Fig. 6. Face of weld of a dissimilar lap weld of AA6016-T4 and 1.4301 [left] and of a dissimilar fillet weld of AA6016-T4 and 1.4301 [right].

### 5.1. Metallographic Analyses

The following section presents the results of the metallographic analyses of the investigated, different dissimilar joints of steel and aluminum alloys. The depiction of the results is divided into two sections, depending on the irradiation side and the arrangement of the base materials in a lap joint (aluminum-sided irradiation, steel-sided irradiation), respectively. The investigations on steel-sidedly laser beam welded different dissimilar joints are shown initially. Afterwards, the results of the metallographic analyses of the aluminum-sidedly welded different dissimilar joints are presented.

The metallographic analyses of dissimilar joints, welded by using a steel-sided irradiation, are shown below for the material pairing of HX220LAD+Z100 ( $t = 1.00$  mm) and AA6016-T4 ( $t = 1.15$  mm) at first. The presented dissimilar welding seams were joined with a varied energy per unit length by using the process parameters denoted in the previous Sec. 3.1. Within the context of these investigations, the variation of the energy per unit length was operated by varying the welding speed  $v$ , while retaining the further process parameters (cf. Sec. 5). Correlating cross-sections of laser beam welded dissimilar joints of HX220LAD+Z100 ( $t = 1.00$  mm) and AA6016-T4 ( $t = 1.15$  mm) with a varied energy per unit length are shown in Fig. 7.

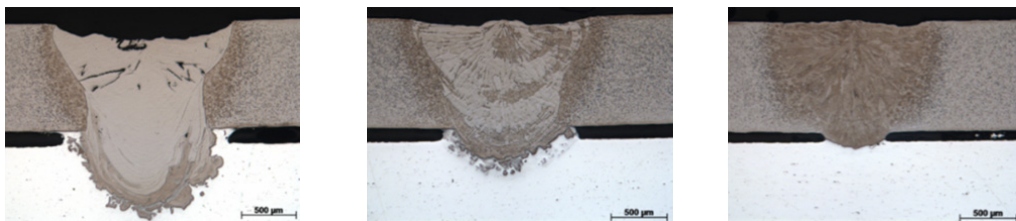


Fig. 7. Cross-sections of laser beam welded dissimilar joints of HX220LAD+Z100 ( $t = 1.00$  mm) and AA6016-T4 ( $t = 1.15$  mm) with a varied energy per unit length of 45.00 kJ/m [left], 43.27 kJ/m [center] and 41.67 kJ/m [right].

In the images of these cross-sections, the upper sheet always consists of the steel material HX220LAD+Z100 ( $t = 1.00$  mm) and was in each cases oriented towards the irradiation direction of the laser beam. The lower positioned joint partner is always a sheet of the aluminum alloy AA6016-T4 ( $t = 1.15$  mm). Overall, the energy per unit length influences the penetration depth  $t_E$  and the weld width  $b$ , whereby the ratio of melted aluminum alloy to melted steel and accordingly the ratio of aluminum to iron in the weld metal is also affected. In Fig. 8 the penetration depth in aluminum alloy  $t_{E, Al}$  and the weld width  $b$  in dependence on the energy per unit length of laser beam welded dissimilar joints of HX220LAD+Z100 ( $t = 1.00$  mm) and AA6016-T4 ( $t = 1.15$  mm) are shown.

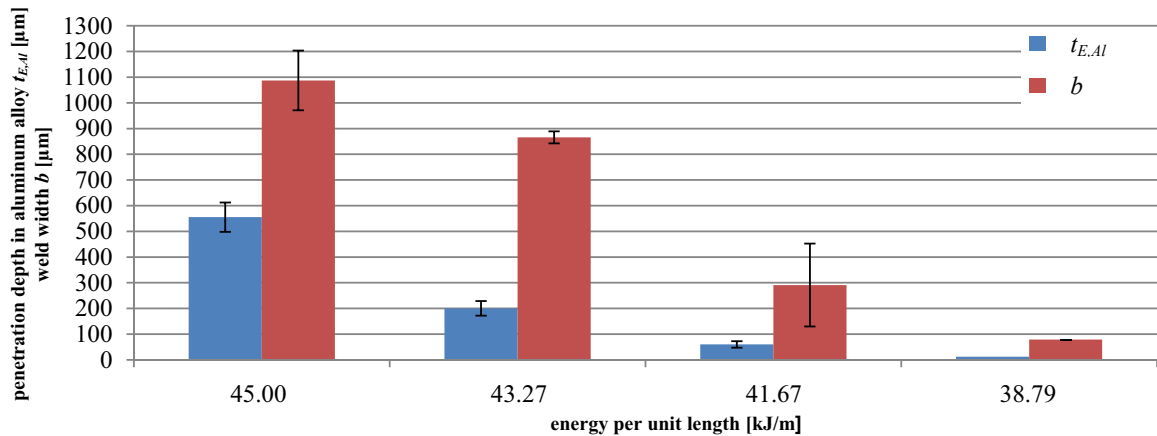


Fig. 8. Penetration depth in aluminum alloy  $t_{E,Al}$  and weld width  $b$  in dependence on the energy per unit length of laser beam welded dissimilar joints of HX220LAD+Z100 ( $t = 1.00$  mm) and AA6016-T4 ( $t = 1.15$  mm).

The penetration depth in aluminum alloy  $t_{E,Al}$ , the weld width  $b$  and according to this the ratio of aluminum to iron in the weld metal increase with an increasing energy per unit length. As a result of an increasing energy per unit length, the aluminum concentration in the weld metal and as a consequence the formation of intermetallic phases also increases. The alteration in the mixing ratio of aluminum to iron in the weld metal in dependence on the energy per unit length are detected by comparing the appearance of the cross-sections shown in Fig. 7. Due to a dependence of the mixing ratio on the appearance of the weld metal in terms of colour as a consequence of an etching process within the scope of a metallographic sample preparation, weld metals joined by using increasing energy per unit length appear in brighter colourations with increasing amounts of light grey areas. Furthermore, the cross-section illustrated in Fig. 7 resulting from an energy per unit length of 45.00 kJ/m is characterized by cracks, especially in the upper third of the weld metal, as a consequence of a relatively high mixing ratio of aluminum to iron in the weld metal.

During the subsequently presented investigations, the steel material as well as the sheet thickness  $t$  of the steel material are varied. Instead of micro-alloyed, fine-grain structural steel, austenitic chromium-nickel steel material was used. Furthermore, the sheet thickness  $t$  of the steel material was increased from 1.00 to 1.50 mm. Due to a distinct increase of the sheet thickness  $t$  of the steel material of 150 %, a higher energy per unit length is necessary for a similar weld shape, although the thermal conductivity of austenitic steels is lower than the thermal conductivity of ferritic steel materials, whereby for austenitic steels by using similar sheet thicknesses  $t$  of the steel materials a lower energy per unit length would be sufficient. In Fig. 9 cross-sections of laser beam welded dissimilar joints of 1.4301 ( $t = 1.50$  mm) and AA6016-T4 ( $t = 1.15$  mm), joined with a varied energy per unit length by using the process parameters denoted in the previous Sec. 3.1, are shown.



Fig. 9. Cross-sections of laser beam welded dissimilar joints of 1.4301 ( $t = 1.50$  mm) and AA6016-T4 ( $t = 1.15$  mm) with a varied energy per unit length of 48.91 kJ/m [left], 46.88 kJ/m [center] and 45.00 kJ/m [right].

Altogether, the energy per unit length influences analogously to the previous material pairing of HX220LAD+Z100 ( $t = 1.00$  mm) and AA6016-T4 ( $t = 1.15$  mm) the penetration depth  $t_{E,Al}$ , the weld width  $b$  and the ratio of aluminum to iron in the weld metal. The relatively high difference in the sheet thickness  $t$  of the steel material and the material properties changed cause among other things a sudden transition from weld-in into the lower positioned joint partner to full penetration with the result that the welding process reacts more sensitive to higher inputs of energy per unit length. This relation may be preferentially attributed to the unfavourable thickness ratio of the metal sheets positioned in a lap joint. As a consequence of an etching process within the scope of a metallographic sample preparation, the intermetallic phases were dissolved out of the weld metal with the result that these areas appear dark on images of corresponding cross-sections. For welding seams with a relatively low penetration depth in aluminum alloy  $t_{E,Al}$ , the intermetallic phases occur mainly in the area of the intermetallic phase seam, which is always positioned in cross-section in vertical direction at the lower border of the weld metal in the sheet of the lower positioned joint partner. In contrast, dissimilar joints with a full penetration of the lower positioned joint partner and according to that with much higher aluminum concentrations in the weld metal and considerably higher amounts of intermetallic phases, respectively, are characterized by over the whole weld metal allocated intermetallic phases, besides the intermetallic phase seam, even though the highest cluster of intermetallic phases is also located in the intermetallic phase seam. Furthermore, the cross-section illustrated in Fig. 9 resulting from an energy per unit length of 48.91 kJ/m is characterized by cracks, especially in the upper half of the weld metal, as a consequence of a relatively high mixing ratio of aluminum to iron in the weld metal. In Fig. 10 the penetration depth in aluminum alloy  $t_{E,Al}$  and the weld width  $b$  in dependence on the energy per unit length of laser beam welded dissimilar joints of 1.4301 ( $t = 1.50$  mm) and AA6016-T4 ( $t = 1.15$  mm) are shown.

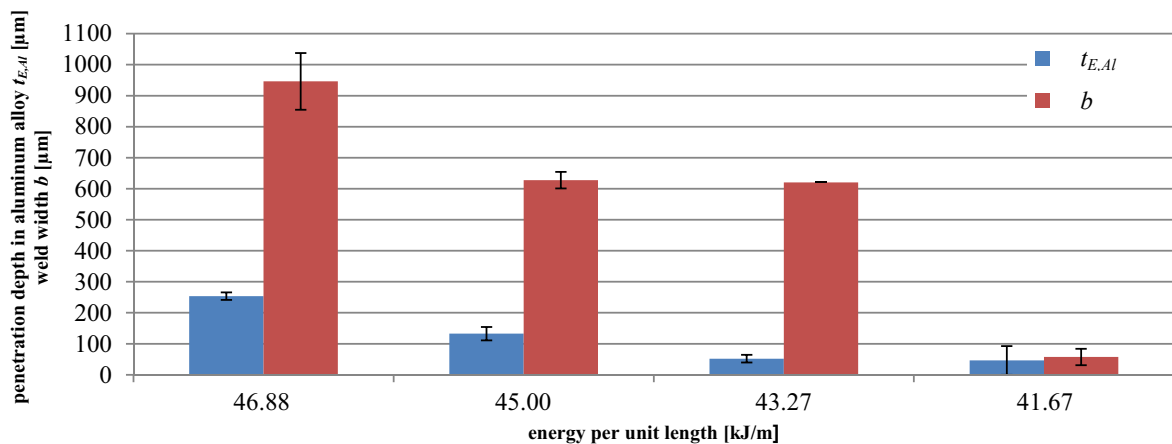


Fig. 10. Penetration depth in aluminum alloy  $t_{E,Al}$  and weld width  $b$  in dependence on the energy per unit length of laser beam welded dissimilar joints of 1.4301 ( $t = 1.50$  mm) and AA6016-T4 ( $t = 1.15$  mm).

Analogously to the previously presented results, an increase of the energy per unit length causes an increase of the penetration depth in aluminum alloy  $t_{E,Al}$ , the weld width  $b$  and according to this of the ratio of aluminum to iron in the weld metal. As a result of an increasing energy per unit length, the aluminum concentration in the weld metal and as a consequence the formation of intermetallic phases also increases. In comparison with the results of the investigations on the previously presented material pairing (cf. Fig. 7 and Fig. 8) of HX220LAD+Z100 ( $t = 1.00$  mm) and AA6016-T4 ( $t = 1.15$  mm) and in consideration of the results of the tensile shear testing, which will be shown in the subsequent section Sec. 5.2, the dissimilar joints of 1.4301 ( $t = 1.50$  mm) and AA6016-T4 ( $t = 1.15$  mm) are characterized by higher weld widths  $b$  for welding seams joined by using an energy per unit length, which is lower than the energy per unit length determined with regard to a maximum for the transmission of tensile shear forces. This relation may be preferentially attributed to the higher sheet thickness  $t$  of the steel material,



whereby a higher energy per unit length is necessary for a full penetration of the upper joint partner, so that as a consequence higher weld widths  $b$  are resulting.

During the subsequently presented investigations, the arrangement of the base materials in a lap joint (irradiation direction) as well as the weld type are varied. Instead of steel-sided irradiation, aluminum-sided irradiation was used. Due to relatively high differences in the material properties of aluminum alloys and steel materials, e. g. higher thermal conductivities, higher reflectivities and accordingly lower absorptivities of radiations with a wavelength  $\lambda$  of 1,030 nm for solid-state aluminum, distinctly higher inputs of energy per unit length are necessary in comparison to the steel-sidedly welded joints. In addition, the weld type was modified from lap weld to fillet weld during the investigations on aluminum-sidedly welded dissimilar joints. The presented results of the investigations on laser beam welding with an aluminum-sided irradiation contain, besides the previously shown material pairings, in addition AA6016-T4 ( $t = 1.15$  mm) and 22MnB5+AS150 ( $t = 1.50$  mm). In Fig. 11 cross-sections of aluminum-sidedly welded dissimilar lap welds of two different material pairings, joined by using an energy per unit length of 125.00 kJ/m and the process parameters denoted in the previous Sec. 3.1, are shown.

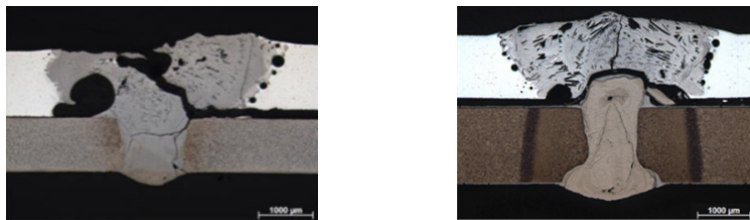


Fig. 11. Cross-sections of dissimilar lap welds of AA6016-T4 ( $t = 1.15$  mm) and HX220LAD+Z100 ( $t = 1.00$  mm) [left] and AA6016-T4 ( $t = 1.15$  mm) and 22MnB5+AS150 ( $t = 1.50$  mm) [right].

In the images of these cross-sections, the upper sheet always consists of the aluminum alloy AA6016-T4 ( $t = 1.15$  mm) and was in each cases oriented towards the irradiation direction of the laser beam. The lower positioned joint partner is in both cases a sheet of the steel material HX220LAD+Z100 ( $t = 1.00$  mm) and 22MnB5+AS150 ( $t = 1.50$  mm), respectively. Especially the areas of the weld metal, positioned in cross-section in vertical direction in the sheet of the upper positioned joint partner, are characterized by cracks with the result of a complete separation of materials in the weld metal, as a consequence of a relatively high mixing ratio of aluminum to iron. Due to the high required inputs of energy per unit length, among other things a sudden transition from insufficient lack of fusion to full penetration of the lower positioned joint partner occurs with the result that the welding process reacts more sensitive to higher inputs of energy per unit length. According to this, a weld-in into the lower positioned joint partner without full penetration was not obtained. Thus, the influence of the energy per unit length on the sensitivity of the aluminum-sidedly laser beam welding process is more distinctly than on the steel-sidedly laser beam welding process, as shown for the previously presented material pairing (cf. Fig. 9 and Fig. 10) of 1.4301 ( $t = 1.50$  mm) and AA6016-T4 ( $t = 1.15$  mm). As soon as the upper positioned sheet of the aluminum alloy obtains full penetration, the lower positioned sheet of the steel material also obtains full penetration, due to the relatively high energy per unit length.

Overall, the welding seams of all the three different material pairings investigated are characterized by very high mixing ratios of aluminum to iron in the weld metal and excessive formation of intermetallic phases and consequently also of cracks. According to this, a lap weld is an unfavourable weld type for the laser beam welding of dissimilar joints of steel and aluminum alloys by using aluminum-sided irradiation. In contrast, fillet welds are much more applicable for this joining assignment, due to the possibilities for a limitation of the amount of melted aluminum alloy and as a consequence for a better control of the mixing ratios of aluminum to iron in the weld metal. Hence, the formation of intermetallic phases and cracks decreases. In Fig. 12 a cross-section of an aluminum-sidedly welded dissimilar fillet weld of AA6016-T4 ( $t = 1.15$  mm) and 1.4301 ( $t = 1.50$  mm), joined by using an energy per unit length of 48.91 kJ/m and the process parameters denoted in the previous Sec. 3.1, is shown.

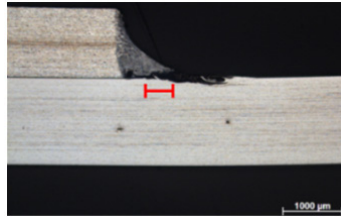


Fig. 12. Cross-section of a dissimilar fillet weld of AA6016-T4 ( $t = 1.15$  mm) and 1.4301 ( $t = 1.50$  mm).

In the image of this cross-section, the upper sheet consists of the aluminum alloy AA6016-T4 ( $t = 1.15$  mm) and was oriented towards the irradiation direction of the laser beam. The lower positioned joint partner is a sheet of the steel material 1.4301 ( $t = 1.50$  mm). Furthermore, the weld width  $b$  is schematically delineated by a red mark in the corresponding image of the cross-section of the dissimilar fillet weld and amounts to about  $500 \mu\text{m}$ . Especially, in the contact area between the dissimilar joint partners or rather in the impact zone of the laser beam, the intermetallic phases occur mainly. In addition, the aluminum-sidedly welded dissimilar fillet welds are characterized by a low occurrence of cracks in the weld metal, as a consequence of the mixing ratio of aluminum to iron in the weld metal.

### 5.2. Tensile Shear Testing

The following section presents the results of the tensile shear testing of the investigated, different dissimilar joints of steel and aluminum alloys. The tensile shear testing contains among other things the determination of tensile shear forces in dependence on the energy per unit length. Analogously to the previously presented results of the metallographic analyses of different dissimilar joints (cf. Sec. 5.1), the depiction of these results is divided into two sections, depending on the irradiation side and the arrangement of the base materials in a lap joint (aluminum-sided irradiation, steel-sided irradiation), respectively. The investigations on steel-sidedly laser beam welded different dissimilar joints are shown initially. Afterwards, the results of the tensile shear testing of the aluminum-sidedly welded different dissimilar joints are presented.

The results of the tensile shear testing of dissimilar joints, welded by using a steel-sided irradiation, are shown below for the material pairing of HX220LAD+Z100 ( $t = 1.00$  mm) and AA6016-T4 ( $t = 1.15$  mm) at first. The presented dissimilar welding seams were joined with a varied energy per unit length by using the process parameters denoted in the previous Sec. 3.1. The corresponding cross-sections of laser beam welded dissimilar joints of HX220LAD+Z100 ( $t = 1.00$  mm) and AA6016-T4 ( $t = 1.15$  mm) with a varied energy per unit length are previously shown in Fig. 7. Within the context of these investigations, the variation of the energy per unit length was operated by varying the welding speed  $v$ , while retaining the further process parameters (cf. Sec. 5). In Fig. 13 the maximum tensile shear force in dependence on the energy per unit length of laser beam welded dissimilar joints of HX220LAD+Z100 ( $t = 1.00$  mm) and AA6016-T4 ( $t = 1.15$  mm) by using different welding speeds  $v$  are shown.

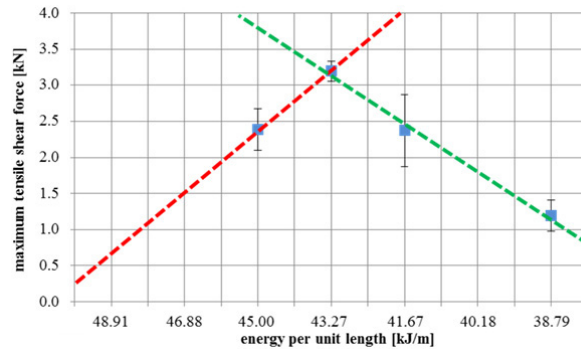


Fig. 13. Maximum tensile shear force in dependence on the energy per unit length of laser beam welded dissimilar joints of HX220LAD+Z100 ( $t = 1.00$  mm) and AA6016-T4 ( $t = 1.15$  mm).

In Fig. 14 the maximum tensile shear force in dependence on the energy per unit length of laser beam welded dissimilar joints of 1.4301 ( $t = 1.50$  mm) and AA6016-T4 ( $t = 1.15$  mm) by using different welding speeds  $v$  are shown.

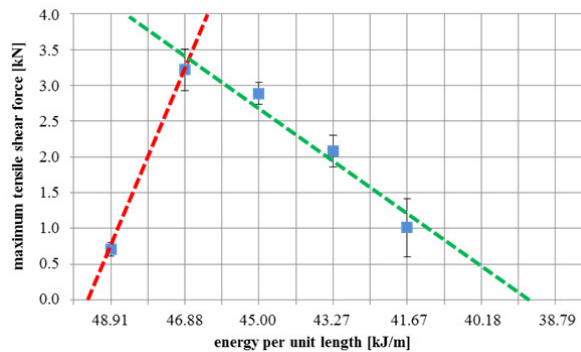


Fig. 14. Maximum tensile shear force in dependence on the energy per unit length of laser beam welded dissimilar joints of 1.4301 ( $t = 1.50$  mm) and AA6016-T4 ( $t = 1.15$  mm).

At first, the penetration depth  $t_E$  and the weld width  $b$  increase with an increasing energy per unit length (cf. Fig. 8 and Fig. 10) for both material pairings of HX220LAD+Z100 ( $t = 1.00$  mm) and AA6016-T4 ( $t = 1.15$  mm) and 1.4301 ( $t = 1.50$  mm) and AA6016-T4 ( $t = 1.15$  mm), respectively. This relation is schematically delineated by a green line in the corresponding Fig. 13 and Fig. 14, respectively. Besides an increasing penetration depth  $t_E$  and weld width  $b$ , as a consequence the ratio of aluminum to iron in the weld metal also increases with an increasing energy per unit length (cf. Fig. 7 and Fig. 9). As a result of an increasing energy per unit length, the aluminum concentration in the weld metal and according to this the formation of intermetallic phases also increases. Thereby, a limitation of the achievable maximum tensile shear forces results, which is schematically delineated by a red line in the corresponding Fig. 13 and Fig. 14, respectively, so that an optimum for the strength of steel-sidedly laser beam welded dissimilar joints is existing. For both material pairings presented, the maximum tensile shear forces of these steel-sidedly laser beam welded dissimilar joints achieved amount to about 3.2 kN (cf. Fig. 13 and Fig. 14). Differences are especially existing with regard to the energy per unit length (46.88 kJ/m and 43.27 kJ/m, respectively), whose joints a maximum for the transmission of tensile shear forces achieved. This relation is among other things preferentially attributed to the relatively high differences in the sheet thickness  $t$  of the steel material (1.50 mm and 1.00 mm, respectively) and the material properties changed.

Due to the results of the metallographic analyses of the dissimilar lap welds (cf. Fig. 11) with regard to high amounts of cracks and complete separation of materials in the weld metal, as a consequence of a relatively high mixing ratio of aluminum to iron in the weld metal, tensile shear testings for this weld type of aluminum-sidedly welded dissimilar joints have not been carried out. In contrast, the aluminum-sidedly welded dissimilar fillet welds were characterized by tensile shear testing. The maximum tensile shear forces for dissimilar fillet welds amounts to about 1.8 kN and were achieved by joints of the material pairing of AA6016-T4 ( $t = 1.15$  mm) and 1.4301 ( $t = 1.50$  mm), joined by using an energy per unit length of 48.91 kJ/m and the process parameters denoted in the previous Sec. 3.1. The weld width  $b$  of these dissimilar fillet welds amounts to about 500  $\mu\text{m}$ . Further investigations on aluminum-sidedly laser beam welding of dissimilar fillet welds by using beam offsets and additionally or separately transverse beam oscillation may increase the weld width  $b$  and as a consequence the achievable maximum tensile shear forces, as far as the alterations will not effectuated an unfavourable increase of the mixing ratio of aluminum to iron in the weld metal.

## 6. Summary and Conclusion

The investigations presented show influences of the energy per unit length, the material grade, the sheet thickness  $t$ , the weld type (lap weld, fillet weld) and the arrangement of the base materials in a lap joint (aluminum-sided irradiation, steel-sided irradiation) on the achievable strengths and the weld shape of different laser beam welded dissimilar joints of steel and aluminum alloys. At first, the penetration depth  $t_E$  and the weld width  $b$  increase with an increasing energy per unit length (cf. Fig. 8 and Fig. 10). Besides an increasing penetration depth  $t_E$  and weld width  $b$ , as a consequence the ratio of aluminum to iron in the weld metal also increases with an increasing energy per unit length (cf. Fig. 7 and Fig. 9). As a result of an increasing energy per unit length, the aluminum concentration in the weld metal and according to this the formation of intermetallic phases also increases. Thereby, a limitation of the achievable maximum tensile shear forces results and amounts to about 3.2 kN (cf. Fig. 13 and Fig. 14). Based on these relations, an obtainment of relatively low penetration depths  $t_E$  in the lower positioned joint partner and as high as possible weld widths  $b$  are advantageously for dissimilar lap joints with regard to a maximum for the transmission of tensile shear forces.

Due to relatively high differences in the material properties of aluminum alloys and steel materials, distinctly higher inputs of energy per unit length are necessary for aluminum-sidedly laser beam welding of dissimilar joints in comparison to steel-sidedly welded joints. Overall, the aluminum-sidedly welded dissimilar lap welds of all the three different material pairings investigated are characterized by very high mixing ratios of aluminum to iron in the weld metal and excessive formation of intermetallic phases and consequently also of cracks (cf. Fig. 11). According to this, a lap weld is an unfavourable weld type for the laser beam welding of dissimilar joints of steel and aluminum alloys by using aluminum-sided irradiation. In contrast, fillet weld are much more applicable for this joining assignment, due to the possibilities for a limitation of the amount of melted aluminum alloy and as a consequence for a better control of the mixing ratios of aluminum to iron in the weld metal. Hence, the formation of intermetallic phases and cracks decreases.

## Acknowledgements

The joint research project "Development of laser based joining technologies for dissimilar lightweight structures" ("Entwicklung von laserbasierten Füge-technologien für artungleiche Leichtbaukonstruktionen", LaserLeichter) is coordinated by Robert Bosch GmbH, held by VDI Technologiezentrum GmbH, and funded by the German Federal Ministry of Education and Research (BMBF).

Furthermore, the authors would like to thank the project partners and the project committee member companies as well as their representatives for supporting the project and for their good cooperation.

## References

- Aichele, G., 2008. Verschweißen von Aluminium mit Stahl. *Industriebedarf* 5-6, 14-16.
- Appel, L., Cramer, H., 2008. Plastisches Fügen von Mischverbindungen mit speziell konturierter Kegelgeometrie. *Schweißen und Schneiden* 60, 12, 691-695.
- Arndt, B., Haage, S., Markus, S., 2013. Umformtechnische Herstellung komplexer Karosserieteile. Springer.
- Büdgam, S., Freitag, V., Hahn, O., Michael, R., 2004. Fügesystemoptimierung für Mischbauweisen im Karosseriebau. *Automobiltechnische Zeitschrift (ATZ)* 106, 12, 1132-1141.
- Council of the European Union, 1993. Council decision of 15 December 1993 concerning the conclusion of the United Nations Framework Convention on Climate Change (94/69/EG).
- Dorn, L., Jafari, S., Hofmann, F., 2003. Ein Vergleich zwischen Laserstrahlschweißen und -löten von Cr-Ni-Stählen. *DVS-Berichte* 225. DVS-Verlag, Düsseldorf, 361-366.
- Horst, F., 2013. *Die Leichtbauwerkstoffe für den Fahrzeugbau*. Springer.
- Jiang, W. H., Kovacevic, R., 2004. Feasibility study of friction stir welding of 6061-T6 aluminium alloy with AISI 1018 steel. *Journal of Engineering Manufacture* 218, 10, 1323-1331.
- Jost, R., Dilger, K., Eberdt, C., 2007. Einsatz der 2K-Technologie bei DaimlerChrysler, *Joining in Automotive Engineering (Automotive Circle International)*. Bad Nauheim, Frankfurt, Germany, 21-27.
- Kaierle, S., Pfeifer, R., Seffer, O., Schimek, M., Bös, J., Bolchoun, A., 2014. Laserstrahlschweißen von Stahl an Aluminium mittels spektroskopischer Kontrolle der Einschweißtiefe und erhöhter Anbindungsbreite durch zweidimensional ausgeprägte Schweißnähte. Final report, AiF-FKZ 378 ZN/1. Forschungsvereinigung Automobiltechnik (FAT), FAT-Schriftenreihe 263.
- Kallage, P., 2013. Laserschweißen von Mischverbindungen aus Aluminium und verzinktem sowie unverzinktem Stahl. Dissertation, Gottfried Wilhelm Leibniz Universität Hannover, PZH Verlag, Garbsen.
- Lau, K., 2006. Nonvakuum-Elektronenstrahlfügen von beschichteten Stahlfeinblechen und Stahl-Aluminium-Mischverbindungen. Dissertation, Gottfried Wilhelm Leibniz Universität Hannover, PZH Verlag, Garbsen.
- Michailov, V. G., Doynov, N., Pfennig, T., Degen, M., Ossenbrink, R., 2011. Simulationsgestützte Entwicklung einer Aluminium-Stahl-Schweißkonstruktion eines Slicermessers für die Lebensmittelverarbeitung. *DVS-Berichte* 275. DVS-Verlag, Düsseldorf, 428-433.
- Müller, M., Wallmann, C., Laukant, H., Glatzel, U., 2005. Prozesstoleranzen des flussmittelfreien Laserstrahlschweißlötens. *Schweißen und Schneiden* 6, 250-255.
- Nothdurft, S., Springer, A., Kaierle, S., Ross, J., Stonis, M., 2016. Laser soldering and brazing of steel-aluminum sheets for tailored hybrid tubes. *Journal of Laser Applications* 28, 2.
- Schilf, M., Wischhusen, B., Thomy, C., Vollertsen, F., Metschkow, B., 2007. Ansätze zum Laserstrahlfügen für Aluminium-Stahl-Verbindungen im Schiffbau. *DVS-Berichte* 244. DVS-Verlag, Düsseldorf, 286-290.
- Schilling, C., Strombeck, A., 2005. Aluminium und Edelstahl vakuumdicht reibrührschweißen. *Blech InForm* 5, 47-49.
- Sierra, G., Peyre, P., Deschaux-Beaume, F., Stuart, D., Fras, G., 2007. Steel to aluminium key-hole laser welding. *Materials Science and Engineering: A*, 447, 1-2, 197-208.
- Staubach, M., Jüttner, S., Füssel, U., Dietrich, M., 2007. Fügen von Stahl-Aluminium-Mischverbindungen mit energiereduzierten MSG-Verfahren und Zusatzwerkstoffen auf Aluminium- und Zinkbasis. *Schweißen und Schneiden* 6, 302-313.
- Thomas, D., Marko, M., Gerson, M., 2004. Kleben und Hybridfügen von Leichtbaustrukturen für den Automobilbau. *Adhäsion Kleben & Dichten* 48, 7, 14-19.
- Thomy, C., Vollertsen, F., Möller, F., Walther, R., 2008. Thermisches Fügen von Mischverbindungen. 6. *Laser-Anwenderforum (LAF)*, Bremen.
- Watanabe, T., Takayama, H., Yanagisawa, A., 2006. Joining of aluminium alloy to steel by friction stir welding. *Journal of Materials Processing Technology* 178, 342-349.